MICROMACHINED ULTRASONIC TRANSDUCERS AND THEIR USE FOR 2D AND 3D IMAGING

B. T. KHURI-YAKUB, A.S. ERGUN, Y. HUANG, C.-H. CHENG, O. ORALKAN, J. JOHNSON, G.G. YARALIOGLU, M. KARAMAN
E. L. Ginzton Laboratory
Stanford University
Stanford, CA 94305-4088

ABSTRACT

Capacitive micromachined ultrasonic transducers (cMUTs) have proven to have remarkable features such as wide bandwidth and high sensitivity allowing the implementation of systems with wide dynamic range. This paper will review the theory and implementation of CMUTs that enable performance that is superior to piezoelectric transducers. In particular, the paper will discuss one-dimensional and two-dimensional arrays, broad frequency of operation (10 kHz to 50 MHz), and high coupling coefficient (k_T^2 value as high as 0.85), and the use of these arrays in imaging applications.
Traditionally, the number of transmit and receive processing channels in a full phased array imaging system is equal to the number of transducers in an ultrasound imaging system. Certain applications limit the number of processing channels such that there are fewer channels than transducer elements. For these cases, phased subarray imaging can be used to reduce the number of transducer elements required for each firing event. Experimental images using the full phased array and phased subarray imaging techniques are compared. Initial results indicate that imaging using subarrays leads to a major reduction in hardware with a small reduction in frame rate and signal to noise ratio.

INTRODUCTION

For over 100 years now, capacitors have been used as transducers for transmitting and receiving sound and ultrasound. Textbooks by Mason [1], Hunt [2], and Beranek [3], to name a few, present theoretical formalisms and in some cases experimental results verifying these theoretical predictions. The performance of these devices has been limited by the relatively low value of electric field in the gap of the capacitor. The advent of silicon micromachining, and micro-electro-mechanical-systems (MEMS) places new capabilities in the design and manufacture of capacitor transducers [4]. It is relatively easy to make capacitors with sub-micron gaps that can handle electric fields of the order of 109 V/m [5,6]. Thus large electro-mechanical coupling and bandwidth

W. Arnold and S. Hirsekorn (eds.), Acoustical Imaging, 1-9.
© 2004 *Kluwer Academic Publishers. Printed in the Netherlands.*

are enabled, which makes capacitor transducers competitive with their piezoelectric counterparts in many applications.

For the details of the simple theory of the parallel plate capacitor transducer, we point the reader to one the fine textbooks mentioned above, or others. In this paper we will present the technology used for making capacitor micromachined ultrasonic transducers (cMUT) and show a number of examples of transducers working at different frequencies, then we will finish by presenting a concept for imaging using a reduced number of RF channels at the expense of some signal to noise and frame rate.

CMUT FABRICATION

Two technologies are used to make cMUTs: sacrificial layer [6] and silicon on insulator bonding [7]. A schematic of the process flow used to make cMUTs by sacrificial layer etching is shown in Fig. 1.

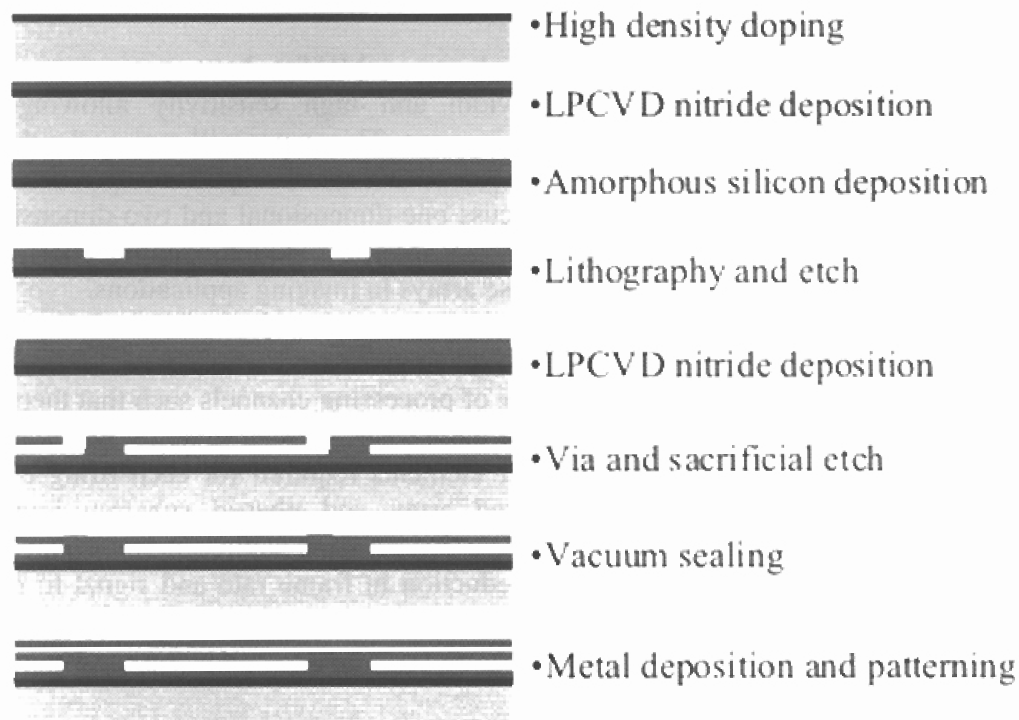

Fig. 1 Schematic of the process flow for making cMUTs by sacrificial layer etching.

In this process, a layer of high doping density is implanted to provide a back electrode for the capacitor. This is followed by the deposition of a thin layer of silicon nitride to protect the conductive layer. The sacrificial layer used in the process is amorphous silicon. The amorphous silicon is deposited to a thickness equal to the gap height of the capacitor. A layer of silicon nitride, which is chosen as the membrane material of the cMUT is deposited over the sacrificial layer. Etch holes are then opened in the silicon nitride to allow the removal of the sacrificial layer by wet etching, then the holes are sealed and an etch back step determines the final thickness of the membrane. Aluminum metal is deposited on the silicon nitride to provide a top electrode, and a sealing layer of

low temperature oxide is then deposited to protect the metal. A picture of a finished device is shown in Fig. 2.

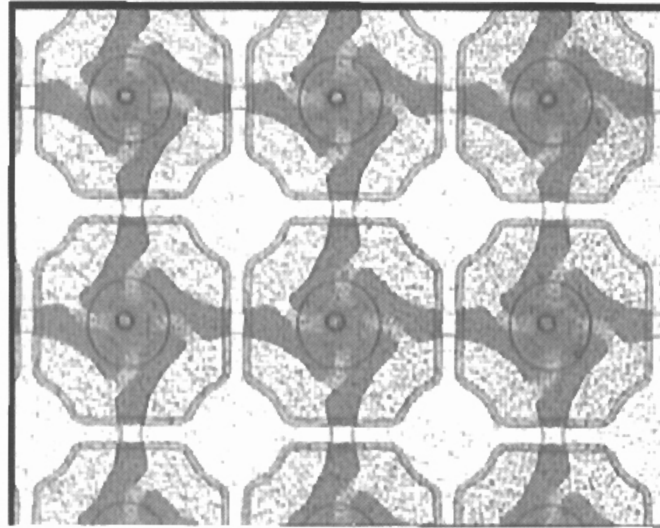

Fig. 2 Picture of a finished cMUT.

Note that in order to achieve high electric fields in the gaps of the cMUT, a transducer is made of many small cells that are connected electrically in parallel. Also, note that the metal electrode covers only half of the membrane of a cell. This is because the outer part of the electrode contributes more parasitic capacitance than acoustic activity.

This above process suffers from difficulty in the control of the thickness of the membrane, its residual stress, its Young's modulus, and the size of the gap. Thus, a silicon on insulator (SOI) bonding process has been developed to overcome these difficulties. The SOI bonding process schedule for making cMUTs is shown in Fig.3.

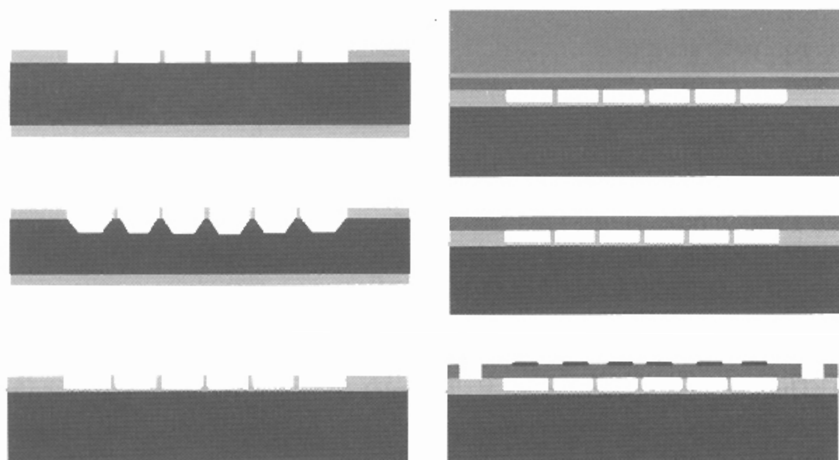

Fig. 3 Schematic of the process flow for making cMUTs by SOI bonding.

In this process, a silicon wafer is oxidized to the height of the gap of the capacitor. The gaps of the capacitors are then defined by photolithography and wet etching. An oxidation step follows to protect the conducting substrate. Next, as SOI wafer is bonded to the previous wafers. Thus, the capacitor cells are all defined and are filled with the vacuum of the bonding step. The carrier of the SOI wafer and oxide are removed to leave a membrane of silicon with the proper thickness over the designed gap. Lastly, the metal is deposited to form the top electrode of the device. A picture of a finished cMUT made by SOI bonding is shown in Fig. 4.

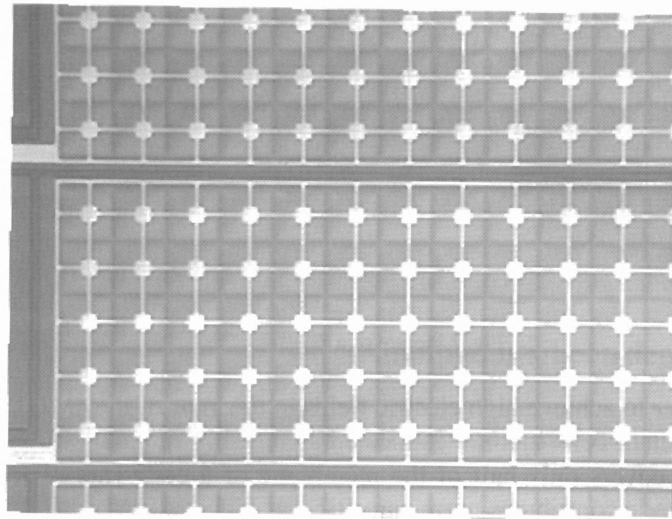

Fig. 4 Picture of a cMUT made by SOI bonding.

In the device of Fig. 4 the individual cells are in the form of a square. Other shapes such as hexagons and rectangles, and of different dimensions, can all be put together to make a transducer.

CMUT PERFORMANCE

a- Single element cMUT

Single element transducers have been made to operate in the frequency range of 10 kHz to 50 MHz. Results for a single element transducer designed to operate in the 400 kHz frequency range will be presented in this section. This transducer is a square 7 mm on the side, and is made of 4900 cells each with a diameter of 94 mm, and a silicon nitride membrane 0.65 mm thick with a gap of 0.1 mm. Figure 5 is the echo signal received from a plane reflector approximately 3.5 cm away in response to a broadband pulse excitation. The DC bias voltage is 40 V. The plot shown with black solid line in Fig. 6 is the Fourier transform of the received signal. The dashed blue line is the calculated two-way loss spectrum including the diffraction and attenuation. Notice that the received signal spectrum and the loss spectrum almost overlap from 100 kHz up to 3

MHz meaning that the frequency spectrum of the CMUT transducer is flat in this frequency range. Figure 7 shows the corrected frequency response of the CMUT transducer. The correction is done by first subtracting the two-way loss spectrum from the Fourier spectrum of the received signal, and then dividing the result by 2 in dB scale. The division by 2 assumes duality in the transmit/receive response, and gives transmit (or receive) frequency spectrum of the CMUT transducer. The result again reveals a broad frequency spectrum from 100 kHz to 3 MHz.

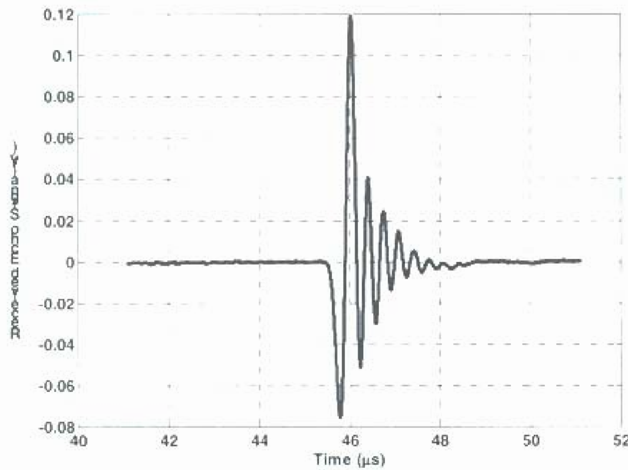

Fig. 5 Pulse-echo response of the cMUT from a flat reflector.

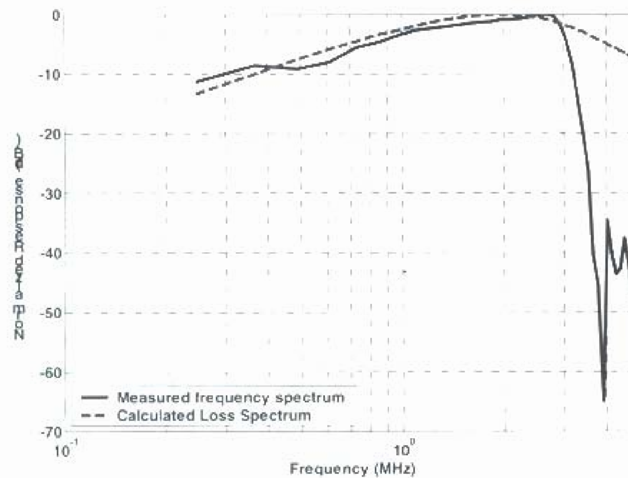

Fig. 6 Frequency spectrum of the echo signal compared to the total (diffraction plus attenuation) loss spectrum.

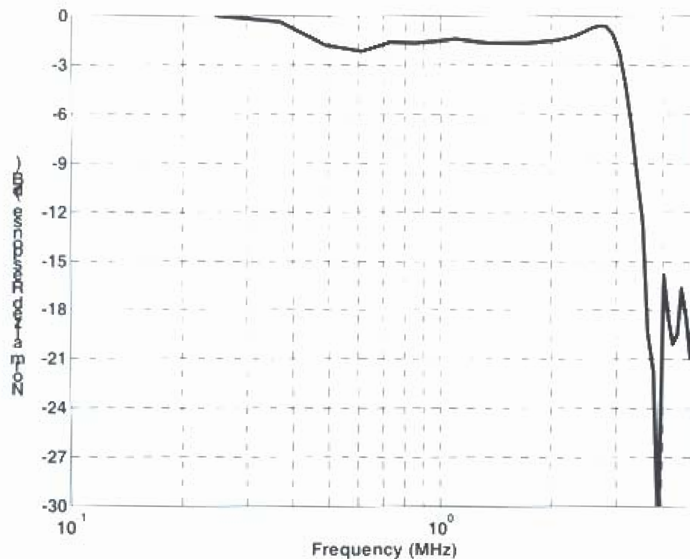

Fig. 7 The corrected frequency response of the CMUT transducer.

A typical feature of cMUTs is the broad frequency range of operation as the upper limit on the frequency of operation is the incidence of the higher order mode of vibration of the membrane. This happens at several multiple of the first order resonance frequency depending on the particular configuration.

b- One-Dimensional and Two-Dimensional arrays

Making 1-D and 2-D arrays is a simple matter of using the proper metal mask while fabricating the transducer. Arrays of hundreds or thousands of elements can be easily implemented on one wafer. The limit on the number of elements is simply the size of the silicon wafer. The performance of the array elements is comparable to that of single element transducers. A typical impulse response and band-shape of a 2-D array element is shown in Fig. 8. The transducer is a square 0.4 mm on the side, with cells that are 36 μm in diameter, and a silicon nitride membrane that is 0.8 μm thick. The transducer element had a measured dynamic range of 130 dB/V/Hz, however that this range can be increased by 10 dB to 20 dB with proper biasing and using better receiver amplifier that is integrated with the transducer. Theoretical calculations indicate that a dynamic range of over 150 dB/V/Hz should be possible with proper design. Note the fractional bandwidth of the transducer is over 100%, a feature that is common to most CMUTs. The measured transducer element was one chosen at random in an array of 128 by 128 elements. All the elements of the array had individual through wafer interconnects that bring contact to the transducer to the backside of the wafer. In this fashion, it is possible to integrate the array with an electronic wafer to reduce the influence of parasitics both on transmit and receive electronic circuitry. Through wafer interconnects have been made with capacitance as low as 0.05 pF and series resistance of the order of 20 Ω [8]. It is possible to use metal filled through wafer interconnects to reduce the resistance to the range of 0.1 Ω if such a low resistance is necessary for device operation.

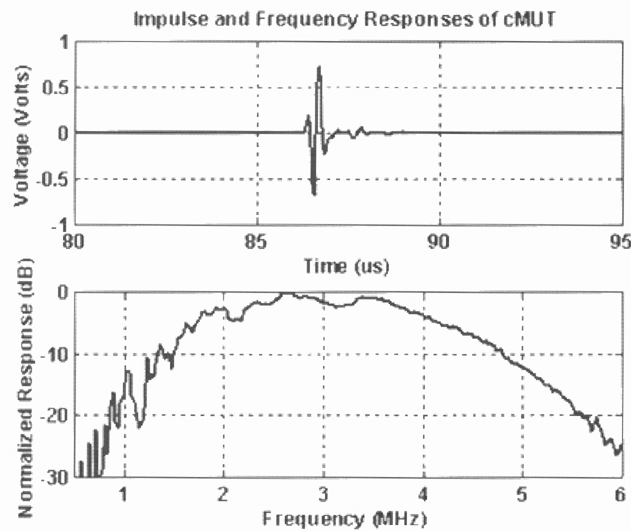

Fig. 8 Impulse response and band-shape of a 2-D array element.

SUB-ARRAY IMAGING AND BEAM FORMING

In conventional full phased array (FPA) imaging, all transducer elements simultaneously transmit properly-delayed pulses to steer and focus an acoustic beam toward a desired location [9-10]. Likewise, all transducer elements simultaneously receive the reflected acoustic signal to form a dynamically focused receive beam. Each transmit/receive "firing event" is repeated, each time steering the beam to a new location. The beams are then combined to form the resultant image.

The proposed phased subarray (PSA) imaging method is based on other studies using synthetic aperture imaging for 2D imaging [11-14]. When applied to 3D imaging, a fully-populated rectangular array is subdivided into a number of overlapping subarrays, each composed of a group of adjacent transducer elements. For each firing event, only a single subarray is used for transmit and receive beamforming. Due to the reduced transmit and receive aperture size, a smaller number of beams need be acquired as determined by the Nyquist sampling criteria without any loss of information. The unacquired beams can be reconstructed by upsampling and interpolation using a subarray-dependent set of filters. Each subarray acquires a different range of spatial frequency components. The spatial frequency range of the combined set of subarrays equals that of the full array. Therefore, by properly weighting the reconstructed subarray images, the response of PSA imaging is equivalent to that of FPA imaging. A full description of this imaging approach is given for 2D imaging in [15], and for 3D imaging in [16].

The performance of this imaging approach as compared to the FPA imaging is shown in Fig. 9. These images were formed using experimental data from a 128-element CMUT array. The phantom consists of six steel wires submersed in a bath of vegetable oil.

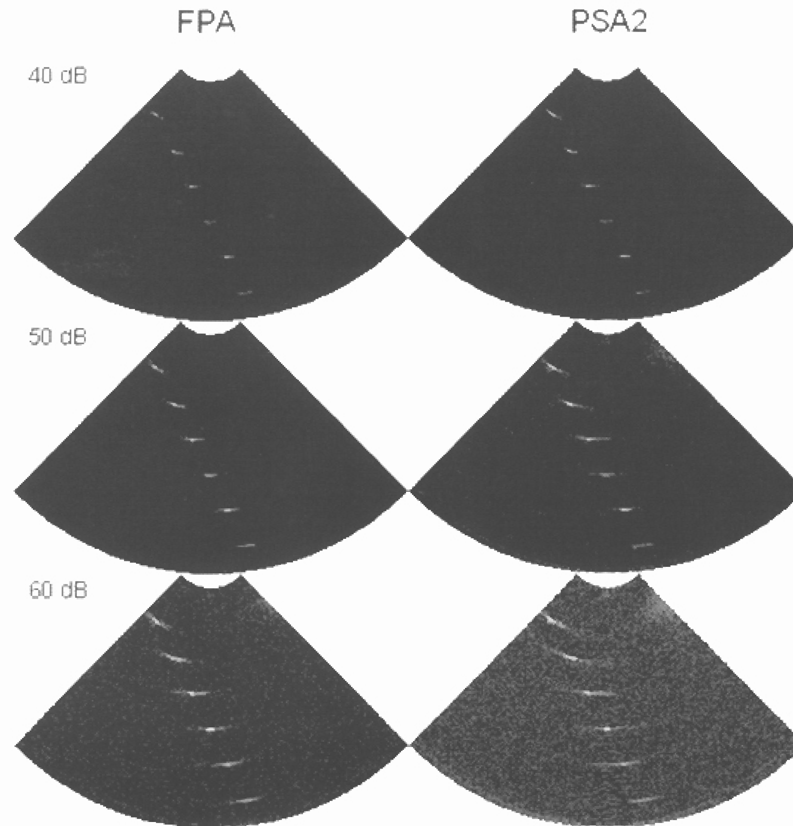

Fig. 9 Comparison of full phased array processing versus subarray processing of a six-wire phantom.

It is seen in Fig. 9 that while there is slight loss in resolution and signal to noise when using subarray processing, there is a net gain in the reduction in complexity of the hardware necessary to implement a system. The FPA images are formed using all 128 elements during each firing event, whereas the PSA2 images are formed use only 32 elements per firing, reducing the hardware complexity by a factor of 4. For an equivalent 3D PSA system, the hardware complexity reduction is even greater, requiring 16 times fewer channels than the corresponding FPA system. This savings is achieved with a slight penalty in the frame rate. Compared to FPA imaging, 2D PSA imaging will reduce the frame rate by at most 2, while 3D PSA imaging reduces the frame rate by at most 4.

CONCLUSIONS

Capacitive micromachined ultrasonic transducers are proving to be an excellent alternative to piezoelectric transducer, especially with regards to bandwidth and to applications where large number of elements are needed in 1-D and 2-D arrays. Processing using sub-arrays is also a viable approach to beam forming if some loss in resolution and signal to noise and frame rate is acceptable in order to reduce the complexity of hardware systems necessary for building small imaging systems.

REFERENCES

[1] W.P. Mason, *Electromechanical Transducers and Wave Filters*, New York, 1942

[2] F.V. Hunt, *Electroacoustics: the analysis of transduction, and its historical background*, Cambridge, Harvard University Press, 1954.

[3] L.L. Beranek, *Acoustics*, Acoustical Society of America, New York, 1993

[4] M.I. Haller and B.T. Khuri-Yakub, "A surface micromachined electrostatic ultrasonic air transducer," *IEEE Trans. Ultrason., Ferroelect., Freq. Contr.*, vol. 43, pp. 1-6, Jan. 1996.

[5] H. T. Soh, I. Ladabaum, A. Atalar, C. F. Quate, and B. T. Khuri-Yakub, "Silicon micromachined ultrasonic immersion transducers," *Appl. Phys. Lett.*, vol. 69, pp. 3674-3676, Dec. 1996.

[6] I. Ladabaum, Xuecheng Jin, H. T. Soh, A. Atalar, and B. T. Khuri-Yakub, "Surface micromachined capacitive ultrasonic transducers," *IEEE Trans. Ultrason., Ferroelect., Freq. Contr.*, vol. 45, pp. 678-690, May 1998.

[7] Yongli Huang, A.S. Ergun, E. Haggstrom, M.H. Badi, B.T. Khuri-Yakub, "Fabricating capacitive micromachined ultrasonic transducers with wafer-bonding technology," *IEEE J. of Microelectromechanicalsystems*, vol. 12, pp. 128-137, April 2003.

[8] C.H. Cheng, A.S. Ergun, B.T. Khuri-Yakub, "Electrical through wafer interconnects with 0.05 pico farads parasitic capacitance on 400 um thick silicon substrate," presented at the Solid-State Sensor, Actuator, and Microsystems Workshop, Hilton Head Island, South Caroline, June 2-6, 2002.

[9] T. A. Shoup and J. Hart, "Ultrasonic imaging systems," presented at IEEE 1988 Ultrasonics Symposium, Chicago, IL, USA, 1988.

[10] B. D. Steinberg, *Principles of Aperture and Array System Design: Including Random and Adaptive Arrays*. New York: Wiley, 1976

[11] C. W. Sherwin, J. P. Ruina, and R. D. Rawcliffe, "Some early developments in synthetic aperture radar systems," *IRE Trans. on Mil. Elec.*, vol. 6, pp. 111-115, 1962.

[12] C. B. Burckhardt, P.-A. Grandchamp, and H. Hoffmann, "Experimental 2 MHz Synthetic Aperture Sonar System Intended for Medical Use," *IEEE Trans. on Son. and Ultrason.*, vol. SU-21, pp. 1-6, 1974.

[13] S. M. Gehlbach and R. E. Alvarez, "Digital ultrasound imaging techniques using vector sampling and raster line reconstruction," *Ultrason. Imag.*, vol. 3, pp. 83-107, 1981.

[14] J. T. Ylitalo and H. Ermert, "Ultrasound synthetic aperture imaging: monostatic approach," *IEEE Trans. Ultrason., Ferroelect., Freq. Contr.*, vol. 41, pp. 333-9, 1994.

[15] J. A. Johnson, M. Karaman, and P. Khuri-Yakub, "Image formation and restoration using multi-element synthetic array processing," Proceedings of SPIE The International Society for Optical Engineering, 2002.

[16] J. A. Johnson, M. Karaman, and B. T. Khuri-Yakub, "Phased subarray processing for underwater 3D acoustic imaging," presented at Oceans '02 MTS/IEEE, 2002.